Journal of Sound and Vibration 546 (2023) 117442

Contents lists available at ScienceDirect

Journal of Sound and Vibration

journal homepage: www.elsevier.com/locate/jsvi

Attenuation band splitting in a finite plate strip with two-dimensional acoustic black holes

Bing Han [a], Hongli Ji [a,*], Li Cheng [b], Wei Huang [c], Jinhao Qiu [a]

[a] State Key Laboratory of Mechanics and Control of Mechanical Structures, Nanjing University of Aeronautics and Astronautics, 29 Yudao Street, Nanjing 210016, China
[b] Department of Mechanical Engineering, Hong Kong Polytechnic University, Hung Hom, Kowloon 999077, Hong Kong
[c] School of Mechanical Engineering, Nanjing University of Science and Technology, Xiaolingwei 200, Nanjing 210094, China

ARTICLE INFO

Keywords:
Acoustic black holes
Bandgap
Finite periodic array
Attenuation band splitting
Resonance mode

ABSTRACT

Acoustic black holes (ABH) lattice is an effective way to realize the bandgaps (BGs) through lightweight design. The predicted BGs using infinitely large periodic structures are commonly believed to enable corresponding attenuation bands (ABs) even the structure only contains a limited number of unit cells. This paper reports an unusual splitting phenomenon in the ABs of a finite plate strip with two-dimensional (2D) ABHs. A wide AB predicted by BG is split into two ABs in the finite strip separated by a high resonance peak, which challenges the aforementioned common belief. Results show that the increasing number of periodic unit cells has a negligible effect on the frequency and amplitude of the resonance peak. Its underlying mechanism is clarified by investigating the relationship between the BGs and ABs, obtained from infinite and finite periodic plate strips with the same 2D ABHs respectively. Complex wavenumber analysis results show the existence of two flexural wave modes in the considered frequency range due to the finite width of the strip. Two types of BGs, in which one satisfies the Bragg condition, are found when both wave modes fail to propagate. Analysis of structural modes further uncover the physical reason for the emerging AB splitting: a certain natural frequency of the boundary portion of the 2D ABHs strip falling into the theoretical BG. Due to the boundary reflection and energy concentration, this structural portion can loosely be regarded as a clamped-free plate strip. It is demonstrated that the resonance peak splitting the AB becomes tunable via disrupting the structural details of finite ABH strips. In particular, extending the terminal end of a finite ABH strip allows the change in boundary portion, which is conducive to eliminating the splitting peak. The reported study is helpful for the design of finite periodic structures with broadband attenuation bandgap.

1. Introduction

Acoustic black hole (ABH) structures have recently attracted increasing attention, which, through effective wave manipulation, enable broadband vibration and noise control applications [1–4]. By tailoring the structural thickness to a power-law variation profile, the ABH acts as a wave trapper to entail a gradual reduction of the phase velocity of flexural waves [5]. As the effect of single ABH is limited by the so-called cut-on frequency [6,7], efforts were made to extend the effective range of ABH to lower frequencies by using

* Corresponding author.
E-mail address: jihongli@nuaa.edu.cn (H. Ji).

https://doi.org/10.1016/j.jsv.2022.117442
Received 12 March 2022; Received in revised form 9 November 2022; Accepted 11 November 2022
Available online 12 November 2022
0022-460X/

ABH lattice structures, inspired by the concept of phononic crystals (PCs) [8–10].

ABH lattice structure was first proposed in one-dimensional (1D) beam structure for prohibiting wave propagation through bandgap (BG) generation [8,11]. Subsequently, various 1D ABH configurations, including folded beams [12], composite ABH beam [13] and annular ABHs [14], were proposed for improving BG performance. More recently, ABHs were embedded into two-dimensional (2D) plates or strips for the same purpose with the consideration of overall structural stiffness [10,15,16]. These works demonstrated that the ABH-induced local resonance and Bragg scattering account for the BG generation in an infinitely large periodic ABH plate, which prohibits wave propagation in both directions.

Realistic structures in practice only contain a limited number of unit cells, contrary to the infinite lattice traditionally used for BG prediction. As such, waves cannot be completely prohibited within the band, although a significant energy attenuation can still be achieved. The corresponding band in the finite lattice offering strong energy attenuation is referred to as attenuation band (AB) [17]. Existing literature has always shown that the two bands, BG and AB, are roughly the same [10,18–21]. This offers a very convenient mean for structural design based on BG analysis. Researches in references [22,23] showed that there exists band-gap resonance phenomenon in a finite lattice design, which indeed influences the effective bandwidth of the BG-predicted AB. However, the mechanism behind remains obscure.

Motivated by this, this works aims at the comparison of the AB of finite plate strip with embedded periodic 2D ABHs and the BG of the infinite counterpart, thus to uncover the potential band-gap resonance phenomenon in a finite 2D ABH lattice and the underlying mechanism. Moreover, the possible strategy for eliminating the so-called band-gap resonance should be investigated to warrant the real broadband attenuation based on periodic ABHs design.

The rest of this paper is structured as follows. The flexural wave BG of an infinite plate strip with periodic 2D ABHs is clarified in Section 2 by scrutinizing the band structure and eigen-mode characteristics. In Section 3, an unusual splitting phenomenon is observed within the AB of a finite plate strip with embedded 2D ABHs. This phenomenon challenges the aforementioned common belief that the finite periodic structure enables ABs with the roughly same width as the bandgaps (BGs) predicted by the infinite counterpart, and also impacts on the common structural design practice. Section 4 uncovers the underlying mechanism of the observed splitting phenomenon by investigating the wave motion characteristics in infinite periodic arrays of ABHs, and also the natural modes of the finite counterparts. Section 5 presents the effective design strategy to overcome the AB splitting for ensuring broad and continuous AB. Finally, conclusions are drawn in Section 6.

2. Flexural wave bandgaps in infinite plate strip with ABHs

As shown in Fig. 1, a plate strip of finite length, consisting of five periodic ABH cells with lattice constant $a = 0.14$ m, is investigated. Each periodic cell contains an ABH indentation with diameter $D = 0.1$ m along the central line of the strip. Taking the center of the ABH as the origin of the local coordinates, the thickness variation along the radial direction of the ABH is defined by

$$h(x) = \begin{cases} h_{\mathrm{m}} & (0 \le x \le r_1) \\ \varepsilon(x - r_1)^2 + h_{\mathrm{m}} & (r_1 \le x \le D/2) \end{cases} \tag{1}$$

where the minimum thickness h_{m} is 0.5 mm; the uniform part of the plate strip is h_{m}=5.18 mm thick; the radius r_1 of the central platform is 10 mm and thus the coefficient ε is 0.0029. The plate is made of aluminum with a mass density of 2820 kg m^{-3}, Poisson ratio of 0.33 and Young modulus of 71 GPa. Using a finite element (FE) model, Floquet periodicity boundary condition is imposed at the two boundaries of the periodic cell, leading to an eigenvalue problem whose solution with a given real wavenumber k yields the band structure.

The condensed band structure is calculated to reveal the flexural wave BG through two processes: (i) the torsional modes are removed, since only flexural waves are considered for the AB generation in such finite ABH plate strip [24]; (ii) considering the coupling between the in-plane and flexural modes, the mode polarization in the z direction is introduced to highlight the flexural modes as:

$$P_w = \frac{\int_V |w|^2 dV}{\int_V \left(|u|^2 + |v|^2 + |w|^2\right) dV} \tag{2}$$

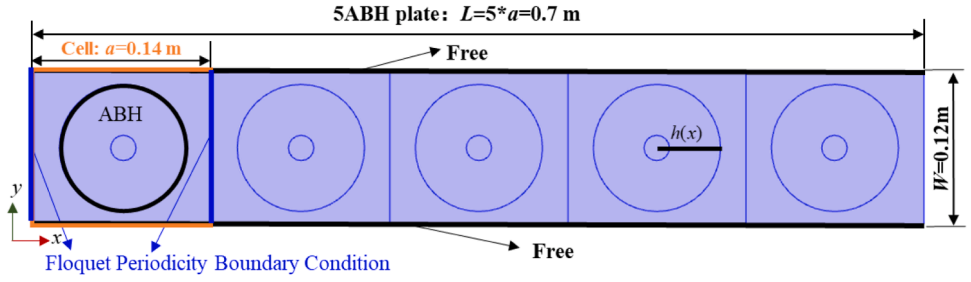

Fig. 1. Finite ABH plate strips consisting of five periodic cells ($N = 5$).

in which u, v and w are the displacement in x, y and z directions, and the integral domain covers the entire material volume V in the periodic cell. Fig. 2 shows the calculated condensed band structure of the periodic ABH and that of the uniform cells by using the $\omega(k)$ method [25,26]. The uniform cell has the same size as the periodic cell in Fig. 1. The greyscale represents the value of P_w and the eigen-modes labeled in Fig. 2 are shown in Fig. 3 for both uniform and ABH periodic cells.

It is obvious that two flexural wave modes propagate along x direction in an infinite uniform strip in the considered frequency range of 0∼5000 Hz, named as BZ0 and BZ1 [24], with the BZ1 mode starting from 2000 Hz. According to the mode shape $\phi_z(y)$ along the left edge of the uniform cell, as shown in Fig. 3, the two modes have different bending deformation along y axis due to the finite width of the strip. The mode BZ0 in Figs. 3(a) and 3(d) [refer to $k = 0.6, f = 1209$ Hz and $k = 0.6, f = 4165$ Hz in Fig. 2(a)] is featured with nearly uniform deformation along y axis (zero order), while the BZ1 in Figs. 3(b) and 3(c) [refer to $k = 0.6, f = 2295$ Hz and $k = 0.6, f = 3589$ Hz in Fig. 2(a)] is the first-order bending mode in the width direction. The band structure of the flexural wave in the periodic ABH strip is more complex. As modes shown in Fig. 3, the waves in the periodic ABH strip are dominated by the two flexural modes, which are also coupled with the in-plane modes. When the in-plane motion of a mode becomes dominant, P_w becomes small, as shown in Fig. 2.

Fig. 2(b) shows four BGs, in which the one around 2200 Hz is insignificant due to the strong coupling between the flexural and in-plane modes. Although all the four BGs are crossed over by the characteristic lines corresponding to the in-plane modes, these in-plane modes do not affect the other three BGs because the out-of-plate displacement of the in-plane modes is small.

3. Attenuation band splitting phenomenon

In order to verify the suitability of using the BGs for the prediction of ABs in the corresponding finite ABH strip, the transmissibility of the finite ABH plate strips containing different numbers of periodic cells is calculated when the strip is subjected to the out-of-plane force at the left side under free boundary conditions. This out-of-plane force is perpendicular to the xy plane (refer to the coordinate system in Fig. 1), and centrally imposed at the left side to facilitate the flexural vibration analysis. The transmissibility is defined as the ratio of the line-averaged flexural displacement amplitude on the receiving side to that on the excitation side [24].

As shown in Fig. 4(a), the ABs with transmissibility smaller than −10 dB generally agree with the predicted BG ranges in Fig. 2(b) with a few exceptions. The most notable exception is that a high transmission peak appears in the BG around 3550 Hz. That is, the BG-predicted wide AB is split into two narrow ABs in the finite strip, a phenomenon which is referred to as AB splitting. The distribution of the out-of-plane response amplitude over a strip with five cells at 3550 Hz is presented in Fig. 4(b). It is obvious that the peak that splits the AB does not shift significantly as the number of unit cells varies, which agrees with the first criterion for the judgment of band-gap resonance in reference [22]. However, the peak value, as shown in Fig. 5, does not always decrease as the number of unit cells increases, which is in contradiction with the second criterion for the judgment of band-gap resonance widely used in the literature. Another transmission peak around 3325 Hz can also be observed within the BG, but only appears in the ABH plate strips when the N is a multiple of 5.

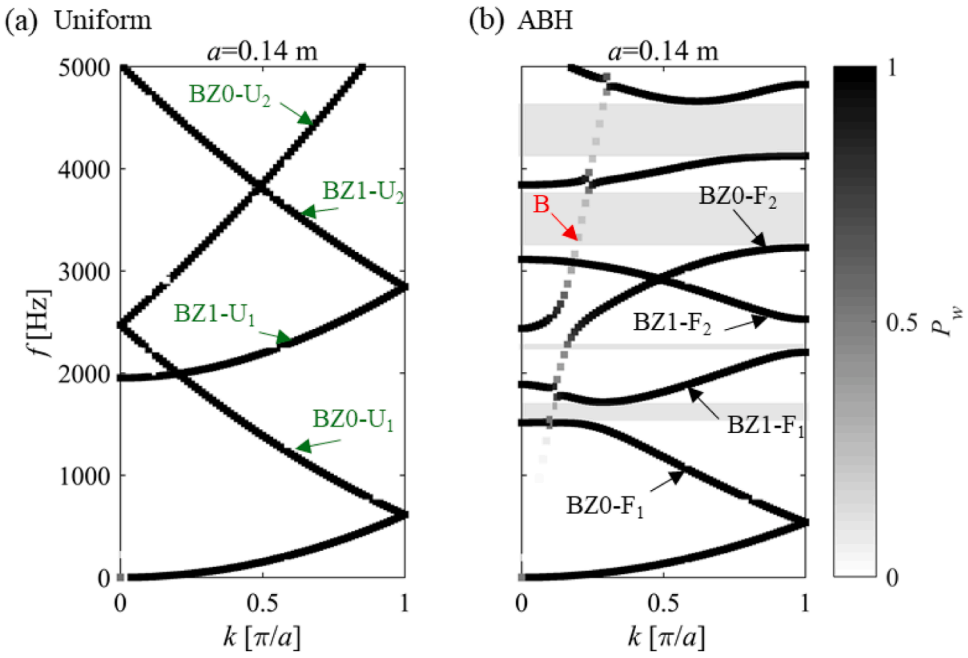

Fig. 2. Condensed band structures of (a) infinite uniform and (b) periodic ABHs strips in the reduced Brillouin zone. gray stripes mark the BGs of the infinite periodic ABH plate strip.

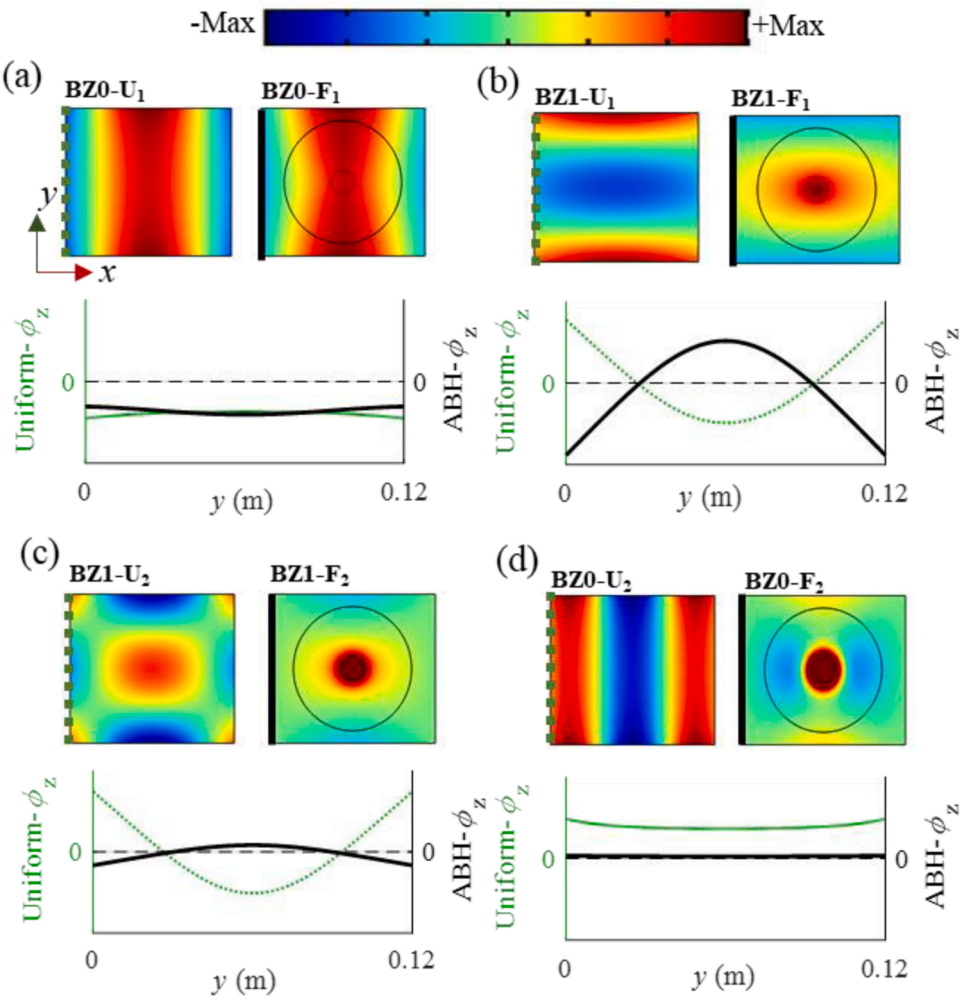

Fig. 3. Representative mode shape of the flexural modes (a)(d) BZ0 and (b)(c) BZ1 for uniform and periodic cells. Dotted lines and solid lines describe the mode shape $\phi_z(y)$ along the left edge of the uniform cell and that of the periodic ABH cell respectively. The thin dashed line marks the zero level.

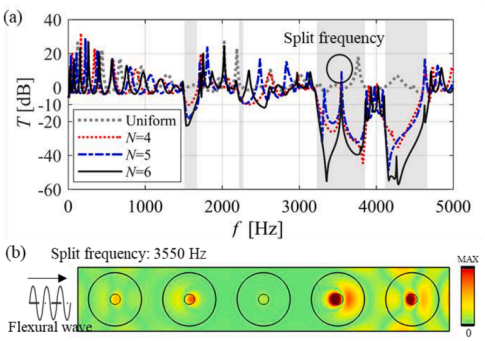

Fig. 4. (a) Transmissibility of finite plate strips with different numbers of periodic ABH cells and the referenced uniform plate; (b) out-plane response amplitude over the ABH plate ($N = 5$) at the splitting frequency.

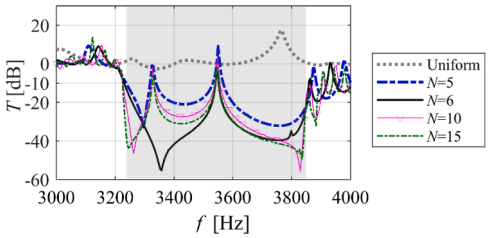

Fig. 5. Narrow-band transmissibility of finite periodic plate strips with $N = 5$, 6, 10 and 15 ABH unit cells.

4. Mechanism analysis and discussions

4.1. Wave motions in infinite system

To understand the unexpected AB splitting phenomenon, the characteristics of the two flexural waves were scrutinized. To this end, the complex band structure shown in Fig. 6 is calculated using $k(\omega)$ method based on FE analysis [27]. The imaginary part of the complex wavenumber k represents the decay rate of the wave during propagation. The larger its absolute value is, the faster the wave decays. Hence, three types of waves can be labeled according to the complex wavenumber [21,28]:

1) Propagating type (P): with a purely real wavenumber, wave propagates without attenuation.
2) Attenuation type (A): with the wavenumber in the form of $n\pi/a + \mathrm{iIm}(k)$, $|\mathrm{Im}(k)| > 0$ and n being integer or zero, wave is attenuated and the wavelength satisfies the Bragg condition. The Bragg condition in a 1D periodic system means that the BG edges occur when $a = n\lambda/2 (n = 1, 2, 3, \ldots)$ with λ being the wavelength [29,30].
3) Complex type (C): with the wavenumber in a general complex form $\mathrm{Re}(k) + \mathrm{iIm}(k)$, $|\mathrm{Re}(k)| \neq n\pi/a$ and $\mathrm{Im}(k) > 0$, wave is attenuated during its propagation.

Only the modes with P_w larger than 0.5 are retained to facilitate the analysis. The real and imaginary parts of the wavenumber are drawn in Figs. 6(a) and (b), respectively. Instead of using the compact form in the reduced Brillouin zone, the extended-zone scheme is used for the real wavenumber curves. The two branches of the real wavenumber curves correspond to the BZ0 and BZ1, respectively. The BZ0 curve starts from 0 Hz and that of the BZ1 mode starts from 1515 Hz for the ABH strip. Unlike the wavenumber curves for the uniform strip, discontinuities appear in the real wavenumber curves of the periodic strip due to the coupling between the flexural and the in-plane modes. The most notable discontinuity appears between points $\overline{6}$ and $\overline{9}$ in the BZ0 branch as shown in Fig. 6(a).

Fig. 6 shows possible combinations of the two flexural modes, namely $\overline{\mathrm{PP}}$, $\overline{\mathrm{AP}}$, $\overline{\mathrm{PA}}$, $\overline{\mathrm{AA}}$ and $\overline{\mathrm{CC}}$, in which the first and second symbols represent the type of BZ0 and BZ1 modes, respectively. If one of the two modes is P-type at a specific frequency, wave can propagate without attenuation in the periodic ABH strip. A BG is formed only when both flexural waves fail to propagate, i.e. only when the

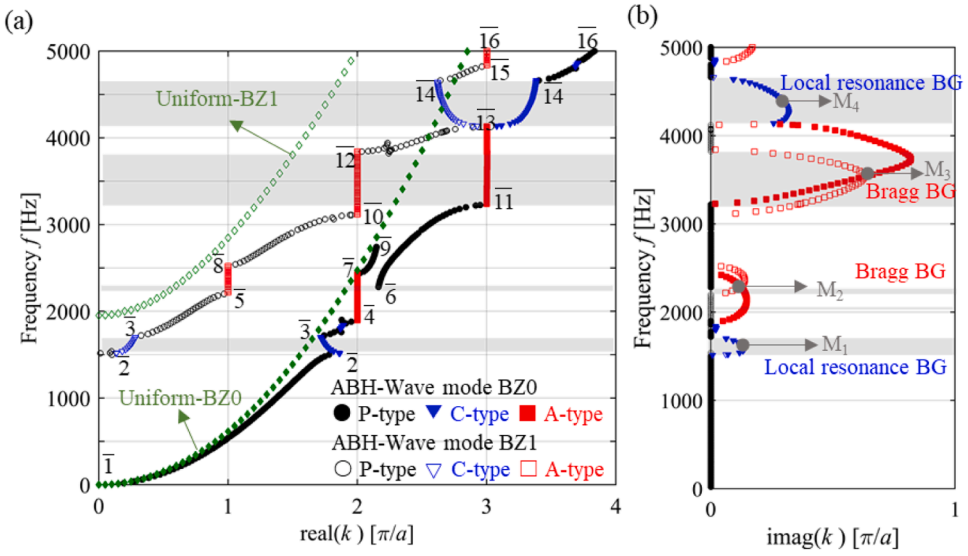

Fig. 6. Complex band structure: (a) The real wavenumber curves corresponding to two flexural modes in the extended-zone scheme for the infinite periodic ABHs and uniform strips. (b) The imaginary wavenumber curves of the infinite periodic ABHs.

combination of mode type is $\overline{AA}$ or $\overline{CC}$. For clarity, the characteristic frequencies corresponding to mode type switching are labeled by $\overline{1}$ to $\overline{16}$ in Fig. 6(a) and are accordingly listed in Table 1. For the four BGs in Fig. 2(b), the two with $\overline{AA}$ combination are called Bragg BGs, since the A-type wave satisfies the Bragg condition. The other two with the $\overline{CC}$ combination without satisfying the Bragg condition are categorized as locally resonant BGs. As the eigen-modes of two evanescent flexural waves shown in Fig. 7, it is observed that the wave motion inside the four BGs is accompanied by the local resonance in the ABH areas, which agrees with the conclusion from a previous study [15].

Fig. 6 shows that in the two locally resonant BGs ($\overline{CC}$ type), the two wave modes have the same Im(k) and the upper and lower frequency bounds of BGs. The frequency ranges of these two BGs agree well with those of the corresponding ABs in Fig. 4(a). As shown in Fig. 4(a), the attenuation effect is enhanced as the number of unit cells increases for all Bragg and local resonance BGs.

For the Bragg BGs ($\overline{AA}$ type), the overlapping frequency interval between the two A-type waves, respectively corresponding to the BZ0 and BZ1 modes, usually determine the Bragg BG range, because the two wave modes have different upper and lower frequencies for the A-type wave. Focusing on the Bragg BG starting from 2200 Hz, the A-type wave of BZ0 mode in Fig. 6 spans the frequency interval from 1880 Hz to 2420 Hz, while that of BZ1 mode is from 2200 Hz to 2520 Hz, thus this Bragg BG should be lower and upper bounded with 2200 Hz and 2420 Hz respectively. However, the theoretical upper bound of the Bragg BG becomes lower due to the coupling between the BZ0 mode and the in-plane modes at $f_{\overline{6}} = 2280$ Hz. This coupling makes it more difficult to visualize this BG in Fig. 3(a) using a small number of unit cells.

The splitting phenomenon occurs on the AB, which should correspond to the BG bounded by the mode BZ0 at the lower frequency 3240 Hz and the mode BZ1 at the upper frequency 3840 Hz. As the upper and lower frequency bounds of the BZ0 mode are both higher than that of the BZ1 mode, the imaginary wavenumber curves of the two modes cross at 3550 Hz inside the Bragg BG, as shown in Fig. 6 (b). The same crossing point also can be found for the Bragg BG around 2200 Hz, but there exists P-type BZ0 mode at this crossing frequency.

In addition, Fig. 6 shows the coupling between the Bragg BG from 3240 Hz to 4130 Hz and the local resonance BG from 4130 Hz to 4660 Hz of the BZ0 mode. This type of BG coupling has been reported as an effective way for achieving broadband AB in locally resonant beams [21,30,31]. However, this BG coupling only exists for the flexural wave BZ0 and fails to generate wide ABs in current situation due to the $\overline{AP}$ combination from 3840 to 4130 Hz. Therefore, the existing two flexural wave modes in such plate configuration would increase the difficulty in broadening the AB based on the exact coupling between two different BGs.

Since Im(k) represents the decaying property of the waves, waves with a positive Im(k) cannot propagate infinitely in a periodic structure. In a finite strip with a small number of ABHs, the wave does not decay to zero, which results in wave reflection from the two structural boundaries. Since $|\mathrm{Re}(k)| = n\pi/a$ with k being computed based on the Bloch-Floquet condition, the wave mode usually does not satisfy the boundary condition in a finite strip. Therefore, resonance of the finite strip usually does not fall into the BG and the transmissibility is usually small due to the wave decaying.

4.2. Natural modes in finite system

The natural mode analysis of the finite ABH plate strip aims at uncovering that special cases of resonance of the finite strip can fall into the BG when some conditions are satisfied. As the natural modes shown in Fig. 8 for finite strips consisting of different numbers of periodic unit cells, every ABH strip has two natural modes falling into the Bragg BG from 3240 Hz to 3840 Hz. Especially, the modes at 3544.8 Hz and 3548.1 Hz of the strip with 6 unit cells and the modes at 3545.1 Hz and 3550.6 Hz of the strip with 10 unit cells show

Table 1
The characteristic frequencies corresponding to mode type switching among P-type, C-type and A-type wave motions, and the frequency intervals of BGs below 5000 Hz.

i	f_i (Hz)	Wave Mode BZ0	BZ1	BG Ranges (Hz)
$\overline{1}$	0	P (0~1515Hz)	None	–
$\overline{2}$	1515	C (1515Hz~1700Hz)	C (1515Hz~1700Hz)	Local resonance: 1515~1700
$\overline{3}$	1700			
$\overline{4}$	1880	P (1700Hz~1880Hz)	P (1700Hz~2200Hz)	–
$\overline{5}$	2200	A (1880Hz~2420Hz)	A (2200Hz~2520Hz)	Bragg:2200~2280
$\overline{6}$	2280			–
$\overline{7}$	2420	P (2420Hz~3240Hz)		
$\overline{8}$	2520		P (2520Hz~3120Hz)	
$\overline{9}$	2740			
$\overline{10}$	3120		A (3120Hz~3840Hz)	
$\overline{11}$	3240	A (3240Hz~4130Hz)		Bragg:3240~3840
$\overline{12}$	3840		P (3840Hz~4130Hz)	–
$\overline{13}$	4130	C (4130Hz~4660Hz)	C (4130Hz~4660Hz)	Local resonance: 4130~4660
$\overline{14}$	4660			
$\overline{15}$	4840	P (4660Hz~5000Hz)	P (4660Hz~4840Hz)	–
$\overline{16}$	5000		A (4840Hz~5000Hz)	

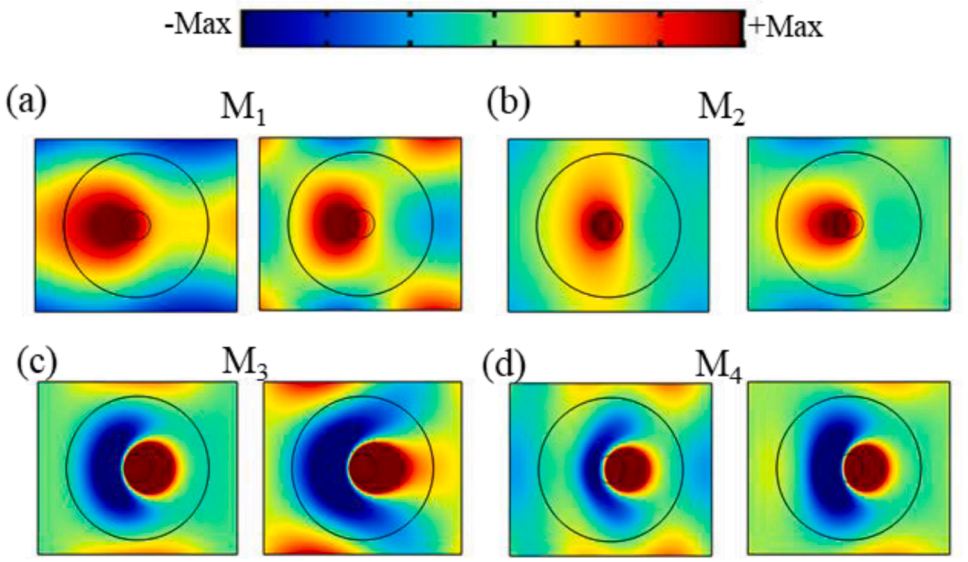

Fig. 7. Eigen-modes in (a)(d) local resonance BGs and (b)(c) Bragg BGs.

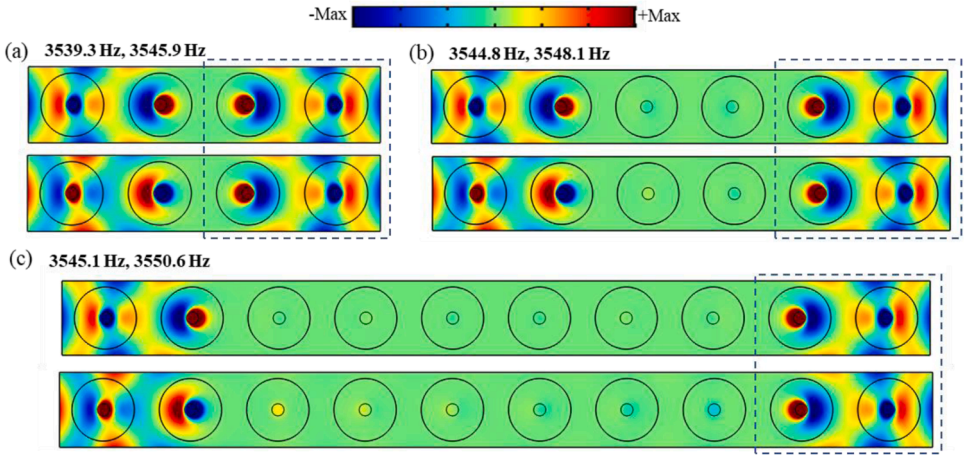

Fig 8. A pair of natural modes around 3550 Hz for finite plates with $N = 4, 6, 10$ periodic ABH cells under free boundary condition.

that the unit cells in the middle part of the strip undergo very low vibration and the two cells at each end bridge the nearly static state in the middle cells to the free boundary condition on the edge. This suggests that the portion of the two boundary unit cells in the strip can be loosely regarded as an independent structure with approximately clamped-free boundary conditions with local standing wave created in this portion of the strip, which can be called boundary portion (see the regions marked by dashed boxes in Fig. 8). To further confirm this explanation, natural modes of the independent plate consisting of two unit cells are calculated with one side clamped and the others free, as shown in Fig. 9(a). Within the frequency range from 3240 Hz to 3840 Hz, one natural mode is found as shown in

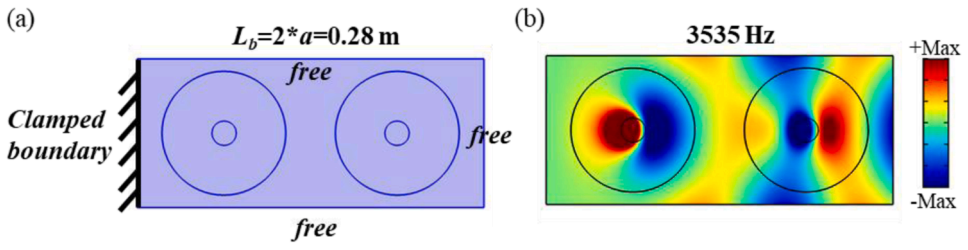

Fig. 9. (a) Clamped-free supported plate with two periodic ABH unit cells and (b) natural mode within a narrow band from 3240 Hz to 3840 Hz.

Fig. 9(b). It is obvious that the mode shape at 3535 Hz of this boundary portion presents the same characteristic as the mode deformation in two boundary unit cells indicated in Fig. 8. Obviously, the necessary condition for the generation of resonance modes which split the AB is that the natural frequency of the boundary portion falls into the corresponding BG. Considering this, it cannot be excluded that the observed AB splitting would appear within the local resonance BG in other situations with different unit cell designs. For the above symmetric strips with length L being a multiple of lattice constant a, the boundary portion with two unit cells satisfies the aforementioned condition.

Therefore, the fact that the resonance mode of a finite periodic design falling into the BG is determined by the natural frequency of the boundary portion also explains why the splitting frequency is not significantly affected by the number of unit cells in the strip. Corresponding to the two wave modes, two resonance modes fall into the BG, as shown in Fig. 8. Because $\mathrm{Re}(k)$ of wave modes BZ1 and BZ0 is 2 and 3, respectively, the two resonance modes have the opposite phase on one side, but the same phase on the opposite side. The transmission peak splitting the wide AB is the resultant effect of the two resonance modes so that it does not always decrease as the number of unit cells increases.

For another resonance peak around 3325 Hz falling into the Bragg BG from 3240 Hz to 3840 Hz only when $N = 5$, 10 and 15 in Fig. 5, modal inspection (not shown here) reveals that this peak is induced by the in-plane wave mode, corresponding to point B in Fig. 2(b) at 3329 Hz. As the velocity of the in-plane wave is larger than the flexural wave, the finite strip with several periods can cover the wavelength of the in-plane wave. With k_u=0.2, the length being 5a matches with half wavelength of the in-plane wave dominated by displacement u, and thus this resonance mode appears in the ABH strip only when the N is a multiple of 5. Due to the in-plane motion domination with P_w=0.18, the peak is not as high as the one at 3550 Hz.

5. Method to tune attenuation band splitting

Since the splitting peak is closely related to the natural mode of the boundary portion with clamped-free supported, the expected way is changing the so-called boundary portion of a plate strip with embedded periodic ABHs. Therefore, to reveal the possibility of tuning the resonance peak and further confirm the aforementioned physical mechanism at the same time, we purposely disrupt the periodicity and the symmetry of the strip by extending its terminal end (right-hand-side uniform part in Fig. 1) by an additional lengthΔL [see the strip in Fig. 10(a)]. Thus the characteristic geometric parameters N_a and L_a of the boundary portion should vary with ΔL. The transmissibility of two strips with different additional lengthΔL is calculated. As the narrow-band results shown in Fig. 10(b), one can see that the transmission peak within the predicted BG can be altered, either reduced (seeΔL=0.05 m) or completely eliminated (seeΔL=0.1 m). Moreover, this change of structural details also eliminates the transmission peak induced by the in-plane wave mode.

According to the above mechanism analysis, resonance modes, which appear in the Bragg BG from 3240 Hz to 3840 Hz, are shown in Fig. 11 for two strips with additional length. It is observed that there still exist two resonance modes for the case ΔL=0.05 m, but only one for ΔL=0.1 m. By scrutinizing the mode shape of caseΔL=0.05 m in Fig. 11(a), it is found that the local standing wave is created in the right one boundary ABH unit cell for the mode at 3520 Hz, but in the left two for the mode at 3547 Hz. For the latter, it is due to the fact that the boundary portion, the natural frequency of which with clamped-free supported falls into the considered BG, consists of two unit cells [cf. Fig. 9(b) and Fig. 11(a)]. Moreover, there exists another boundary portion [see the region marked by the dashed box in Fig. 11(a)] consisting of one unit cell and additional length ΔL=0.05 m, which has one natural mode at 3523 Hz (mode shape not shown here). The resonance mode at 3520 Hz therefore appears in the BG for the five-ABHs strip with ΔL=0.05 m, and thus splits the AB at the different frequency from the five-ABHs strip with ΔL=0.

For the five-ABHs strip with ΔL=0.1 m, there only exists the boundary portion shown in Fig. 9(b) satisfying the aforementioned conditions. Therefore, the AB splitting is eliminated in Fig. 10 duo to the created local standing wave only in the left two boundary unit cells of the strip. This above analysis concludes that geometrically disrupting the periodicity and the symmetry of the strip can mitigate the AB splitting, because the boundary portion varies in different structures. Therefore, we cannot exclude other alternative methods of geometrical disruption, eg. moving ABHs or modifying the profile of ABH near the end with maintaining the structural size. Note that possible rules to achieve prescribed target should be another complex problem of structural design, which requires deeper analysis and is beyond the focus of this work.

6. Conclusions

By analyzing the BG of an infinite periodic ABH plate strip and the transmissibility of the finite counterpart, this work illustrates an unusual splitting phenomenon in the ABs of such finite strip configuration. Analysis on eigen-modes reveals that two types of flexural wave modes are enabled within the frequency range under consideration due to the finite width of the strip. BGs are generated when both wave modes fail to propagate. Therefore, the strategy for realizing ultra-wide continuous AB through coupling the local resonance and Bragg BGs is challenged, due to the difficulty in simultaneously guaranteeing the exact coupling between the two types of BGs for both flexural waves.

The revealed AB splitting phenomenon, with the appearance of a high energy transmission peak, disrupts the BG-predicted broadband and continuous ABs in the strip of finite size, which are usually assumed to coincide with the BG obtained from the band analyses on the corresponding infinite counterpart. Complex wavenumber analysis shows that there exist two kinds of BGs, in which one satisfies the Bragg condition. By scrutinizing the resonance mode characteristic of finite ABH strips, the results uncover the underlying mechanism of AB splitting: the emerging resonance peak within the BG-predicted AB as the results of a natural frequency of the boundary portion of the finite strip falling into the corresponding BG. The so-called boundary portion obviously depends on

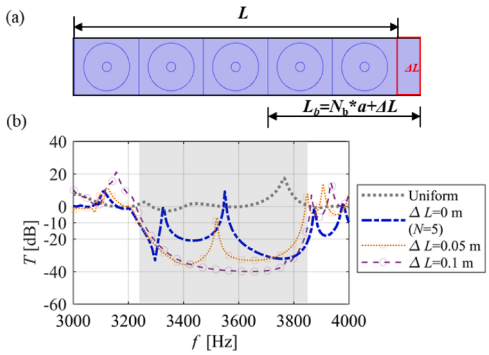

Fig. 10. Narrow-band transmissibility of finite plate strips combining $N = 5$ unit cells with an extension of different length ΔL.

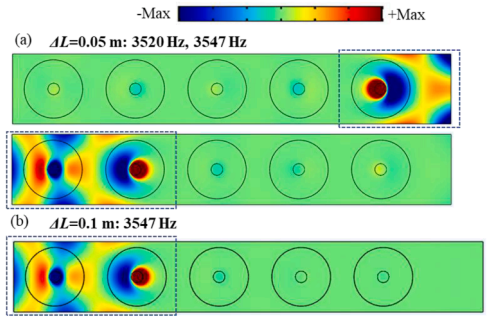

Fig. 11. Resonance modes of finite plate strips combining $N = 5$ unit cells with an extension of different length ΔL= (a) 0.05 m and (b) 0.1 m within a narrow band from 3240 Hz to 3840 Hz.

structural details, so that it is impractical to eliminate the resonance peak by merely increasing the number of periodic unit cells.

Analysis results have confirmed that geometrically disrupting the periodicity and symmetry of the finite periodic ABH plate strip turns out to be an effective way to overcome the challenge of the AB splitting for truly achieving broad and continuous ABs in practice. In particular, as confirmed in this work, by extending the terminal end with different, the splitting peak occurring in the considered finite ABH strip would be reduced or even eliminated. This work offers an understanding on the formation mechanism of the splitting peak within the BG region in a finite structure, and permits avoiding the occurrence of such phenomenon to achieve broadband energy attenuation in practical design.

CRediT authorship contribution statement

Bing Han: Conceptualization, Data curation, Writing – original draft. **Hongli Ji:** Investigation, Formal analysis, Writing – review & editing. **Li Cheng:** Methodology, Writing – review & editing. **Wei Huang:** Validation, Visualization. **Jinhao Qiu:** Methodology, Supervision, Funding acquisition, Project administration.

Declaration of Competing Interest

The authors declare no conflict of interest.

Data Availability

Data will be made available on request.

Acknowledgements

This work is partially supported by the National Key Research and Development Program of China (No. 2021YFB3400100), the National Natural Science Foundation of China (Nos. 52022039, U2241261, 52105107), the Research Fund of State Key Laboratory of Mechanics and Control of Mechanical Structures (Nanjing University of Aeronautics and astronautics, Nos. MCMS-I-0521G03 & MCMS-E-0521Y01), Research Project of State Key Laboratory of Mechanical System and Vibration (No. MSV202220) and a Project

Funded by the Priority Academic Program Development of Jiangsu Higher Education Institutions.

References

[1] A. Pelat, F. Gautier, S.C. Conlon, F. Semperlotti, The acoustic black hole: a review of theory and applications, J. Sound Vib. 476 (2020), 115316, https://doi.org/10.1016/j.jsv.2020.115316.

[2] Y. Mi, W. Zhai, L. Cheng, C. Xi, X. Yu, Wave trapping by acoustic black hole: simultaneous reduction of sound reflection and transmission, Appl. Phys. Lett. 118 (2021), 114101, https://doi.org/10.1063/5.0042514.

[3] T. Durand-Texte, A. Pelat, G. Penelet, F. Gautier, M. Sécail-Géraud, Thermal imaging of vibrational energy dissipated in a 2D acoustic black hole pit, Appl. Phys. Lett. 118 (2021) 13901, https://doi.org/10.1063/5.0030983.

[4] C. Zhao, J. Zheng, T. Sang, L. Wang, Q. Yi, P. Wang, Computational analysis of phononic crystal vibration isolators via FEM coupled with the acoustic black hole effect to attenuate railway-induced vibration, Constr. Build. Mater. 283 (2021), 122802, https://doi.org/10.1016/j.conbuildmat.2021.122802.

[5] W. Huang, H. Ji, J. Qiu, L. Cheng, Wave energy focalization in a plate with imperfect two-dimensional acoustic black hole indentation, J. Vib. Acoust. Trans. ASME. 138 (2016) 61004, https://doi.org/10.1115/1.4034080.

[6] L. Tang, L. Cheng, Enhanced Acoustic Black Hole effect in beams with a modified thickness profile and extended platform, J. Sound Vib. 391 (2017) 116–126, https://doi.org/10.1016/j.jsv.2016.11.010.

[7] L. Tang, L. Cheng, Loss of acoustic black hole effect in a structure of finite size, Appl. Phys. Lett. 109 (2016) 14102, https://doi.org/10.1063/1.4955127.

[8] L. Tang, L. Cheng, Ultrawide band gaps in beams with double-leaf acoustic black hole indentations, J. Acoust. Soc. Am. 142 (2017) 2802–2807, https://doi.org/10.1121/1.5009582.

[9] X. Lyu, Q. Ding, T. Yang, Merging phononic crystals and acoustic black holes, Appl. Math. Mech. (English Ed. 41 (2020) 279–288, https://doi.org/10.1007/s10483-020-2568-7.

[10] J. Deng, L. Zheng, N. Gao, Broad band gaps for flexural wave manipulation in plates with embedded periodic strip acoustic black holes, Int. J. Solids Struct. 224 (2021), 111043, https://doi.org/10.1016/j.ijsolstr.2021.111043.

[11] L. Tang, L. Cheng, Broadband locally resonant band gaps in periodic beam structures with embedded acoustic black holes, J. Appl. Phys. 121 (2017), 194901, https://doi.org/10.1063/1.4983459.

[12] N. Gao, Z. Wei, H. Hou, A.O. Krushynska, Design and experimental investigation of V-folded beams with acoustic black hole indentations, J. Acoust. Soc. Am. 145 (2019) EL79–EL83, https://doi.org/10.1121/1.5088027.

[13] N. Gao, Z. Wei, R. Zhang, H. Hou, Low-frequency elastic wave attenuation in a composite acoustic black hole beam, Appl. Acoust. 154 (2019) 68–76, https://doi.org/10.1016/j.apacoust.2019.04.029.

[14] J. Deng, O. Guasch, L. Maxit, L. Zheng, Reduction of Bloch-Floquet bending waves via annular acoustic black holes in periodically supported cylindrical shell structures, Appl. Acoust. 169 (2020), 107424, https://doi.org/10.1016/j.apacoust.2020.107424.

[15] L. Tang, L. Cheng, K. Chen, Complete Sub-wavelength flexural wave band gaps in plates with periodic acoustic black holes, J. Sound Vib. 502 (2021), 116102, https://doi.org/10.1016/j.jsv.2021.116102.

[16] J. Deng, L. Zheng, O. Guasch, H. Wu, P. Zeng, Y. Zuo, Gaussian expansion for the vibration analysis of plates with multiple acoustic black holes indentations, Mech. Syst. Signal Process. 131 (2019) 317–334, https://doi.org/10.1016/j.ymssp.2019.05.024.

[17] J. Llinares, M. Holgado, Rayleigh-wave attenuation by a semi-infinite two-dimensional elastic-band-gap crystal, Phys. Rev. B - Condens. Matter Mater. Phys. 59 (1999) 12169–12172, https://doi.org/10.1103/PhysRevB.59.12169.

[18] J. Deng, L. Zheng, N. Gao, Broad band gaps for flexural wave manipulation in plates with embedded periodic strip acoustic black holes, Int. J. Solids Struct. 224 (2021), 111043.

[19] L. Tang, N. Gao, J. Xu, K. Chen, L. Cheng, A light-weight periodic plate with embedded acoustic black holes and bandgaps for broadband sound radiation reduction, J. Acoust. Soc. Am. 150 (2021) 3532–3543, https://doi.org/10.1121/10.0007067.

[20] N. Gao, B. Wang, K. Lu, H. Hou, Complex band structure and evanescent Bloch wave propagation of periodic nested acoustic black hole phononic structure, Appl. Acoust. 177 (2021), 107906, https://doi.org/10.1016/j.apacoust.2020.107906.

[21] Y. Xiao, J. Wen, D. Yu, X. Wen, Flexural wave propagation in beams with periodically attached vibration absorbers: band-gap behavior and band formation mechanisms, J. Sound Vib. 332 (2013) 867–893, https://doi.org/10.1016/j.jsv.2012.09.035.

[22] Y. Xiao, J. Wen, G. Wang, X. Wen, Theoretical and experimental study of locally resonant and bragg band gaps in flexural beams carrying periodic arrays of beam-like resonators, J. Vib. Acoust. Trans. ASME. 135 (2013) 41006, https://doi.org/10.1115/1.4024214.

[23] B.L. Davis, A.S. Tomchek, E.A. Flores, L. Liu, M.I. Hussein, Analysis of periodicity termination in phononic crystals, ASME 2011 Int. Mech. Eng. Congr. Expo. IMECE 2011 8 (2011) 973–977, https://doi.org/10.1115/imece2011-65666.

[24] H. Ji, B. Han, L. Cheng, D.J. Inman, J. Qiu, Frequency attenuation band with low vibration transmission in a finite-size plate strip embedded with 2D acoustic black holes, Mech. Syst. Signal Process. 163 (2022), 108149, https://doi.org/10.1016/j.ymssp.2021.108149.

[25] B.R. Mace, E. Manconi, Modelling wave propagation in two-dimensional structures using finite element analysis, J. Sound Vib. 318 (2008) 884–902, https://doi.org/10.1016/j.jsv.2008.04.039.

[26] E. Manconi, S. Sorokin, On the effect of damping on dispersion curves in plates, Int. J. Solids Struct. 50 (2013) 1966–1973, https://doi.org/10.1016/j.ijsolstr.2013.02.016.

[27] Y.F. Wang, Y.S. Wang, V. Laude, Wave propagation in two-dimensional viscoelastic metamaterials, Phys. Rev. B - Condens. Matter Mater. Phys. 92 (2015), 104110, https://doi.org/10.1103/PhysRevB.92.104110.

[28] D.J. Mead, Wave propagation and natural modes in periodic systems: II. Multi-coupled systems, with and without damping, J. Sound Vib. 40 (1975) 19–39, https://doi.org/10.1016/S0022-460X(75)80228-8.

[29] Z. Liu, C.T. Chan, P. Sheng, Three-component elastic wave band-gap material, Phys. Rev. B. 65 (2002), 165116, https://doi.org/10.1103/PhysRevB.65.165116.

[30] Y. Xiao, B.R. MacE, J. Wen, X. Wen, Formation and coupling of band gaps in a locally resonant elastic system comprising a string with attached resonators, Phys. Lett. Sect. A Gen. At. Solid State Phys. 375 (2011) 1485–1491, https://doi.org/10.1016/j.physleta.2011.02.044.

[31] B. Sharma, C.T. Sun, Local resonance and Bragg bandgaps in sandwich beams containing periodically inserted resonators, J. Sound Vib. 364 (2016) 133–146, https://doi.org/10.1016/j.jsv.2015.11.019.